.

IR+vacuum ultraviolet (118 nm) nonresonant ionization spectroscopy of methanol monomers and clusters: Neutral cluster distribution and size-specific detection of the OH stretch vibrations

H. B. Fu, Y. J. Hu, and E. R. Bernstein

IR+vacuum ultraviolet (118 nm) nonresonant ionization spectroscopy of methanol monomers and clusters: Neutral cluster distribution and size-specific detection of the OH stretch vibrations

H. B. Fu, Y. J. Hu, and E. R. Bernstein[a)]
Department of Chemistry, Colorado State University, Fort Collins, Colorado 80523

Small methanol clusters are formed by expanding a mixture of methanol vapor seeded in helium and are detected using vacuum UV (vuv) (118 nm) single-photon ionization/linear time-of-flight mass spectrometer (TOFMS). Protonated cluster ions, $(CH_3OH)_{n-1}H^+$ (n=2–8), formed through intracluster ion-molecule reactions following ionization, essentially correlate to the neutral clusters, $(CH_3OH)_n$, in the present study using 118 nm light as the ionization source. Both experimental and Born-Haber calculational results clarify that not enough excess energy is released into protonated cluster ions to initiate further fragmentation in the time scale appropriate for linear TOFMS. Size-specific spectra for $(CH_3OH)_n$ (n=4 to 8) clusters in the OH stretch fundamental region are recorded by IR+vuv (118 nm) nonresonant ion-dip spectroscopy through the detection chain of IR multiphoton predissociation and subsequent vuv single-photon ionization. The general structures and gross features of these cluster spectra are consistent with previous theoretical calculations. The lowest-energy peak contributed to each cluster spectrum is redshifted with increasing cluster size from n=4 to 8, and limits near ~3220 cm^{-1} in the heptamer and octamer. Moreover, IR+vuv nonresonant ionization detected spectroscopy is employed to study the OH stretch first overtone of the methanol monomer. The rotational temperature of the clusters is estimated to be at least 50 K based on the simulation of the monomer rotational envelope under clustering conditions. © *2006 American Institute of Physics.* [DOI: 10.1063/1.2141951]

I. INTRODUCTION

Hydrogen-bonded clusters have attracted a great deal of interest in recent years,[1,2] largely owing to the concerted effort underway to characterize the behavior of condensed-phase water.[3,4] Methanol clusters represent an important complementary class of hydrogen-bonded systems to water clusters, but are less studied. In contrast to water with its unique ability to form tetrahedrally bonded networks, methanol molecules interact most strongly through one nearly linear hydrogen bond and through hydrophobic (van der Waals) forces around the methyl group.[5–8] An x-ray-diffraction study suggested that methanol molecules in the liquid phase form chainlike structures and, to a lesser extent, also rings with two hydrogen bonds for every molecule.[9] IR spectroscopy of neutral methanol clusters in the gas phase, $(CH_3OH)_n$ (n=2–9), demonstrated that the clusters of n=3 to 9 have cyclic structures in order to maximize the number of hydrogen bonds in the cluster.[10–15] A study of mixed clusters, benzene/$(CH_3OH)_n$ (n=1–6), showed that the methanol moiety maintains a cyclic structure, though the hydrogen-bonded ring is distorted for n≥3 clusters in order to solvate the aromatic molecule.[16–18] In the case of protonated methanol clusters, $(CH_3OH)_{n-1}H^+$, the formation of a bicyclic structure is confirmed in n≥8 clusters.[19]

The OH stretch vibration has been proven to be a sensitive indicator of the hydrogen bond in methanol clusters.

Experimentally, the OH stretch energy is measured by various direct absorption techniques, including matrix isolation IR spectroscopy,[20,21] cavity ringdown laser absorption spectroscopy,[22] Fourier transform IR (FTIR) spectroscopy combined with pulsed slit-jet expansion,[23] and additionally by molecular-beam depletion combined IR photodissociation spectroscopy.[10–15] All direct absorption measurements are not size selected, and only work best for the n≤4 $(CH_3OH)_n$ clusters, for which the spectra themselves can be used to identify the cluster size based on calculations.[22,23] For n≥5 $(CH_3OH)_n$ clusters, the identification of a specific transition with a specific cluster size has to be carried out by a size-selected or size-specific measurement. The molecular-beam depletion method separates $(CH_3OH)_n$ clusters physically from each other, based on the scattering of $(CH_3OH)_n$ species by a helium beam in a high-resolution crossed beam arrangement.[10–15] Zwier and co-workers utilize resonant two-photon ionization of benzene molecules to achieve a size-specific measurement in benzene/$(CH_3OH)_n$ clusters. In this case, the excitation of a suitable electronic state of benzene can be made size specific, and fragmentation is avoided by carefully adjusting the ionization energy near the threshold region.[16–18]

Primary alcohol clusters are very difficult to ionize without fragmentation as a result of intracluster ion-molecule reactions.[24,25] Instead of producing the parent ion, $(ROH)_n^+$, conventional ionization techniques, such as electron impact[26–28] (EI) and UV multiphoton ionization (MPI),[29–31]

[a)]Electronic mail: erb@lamar.colostate.edu

generally yield $(ROH)_{n-3}H_3O^+$ and $(ROH)_{n-1}H^+$ cluster ions, since significant excess energy is imparted to cluster ions during the ionization processes associated with these techniques. The neutral cluster distribution is lost in these instances. Our previous studies on metal oxide clusters demonstrate that a 118 nm vacuum ultraviolet (vuv) single laser photon provides a nonresonant soft ionization source; that is, one for which cluster fragmentation is minimized during the ionization process.[32,33] In an early study using vuv synchrotron radiation as an ionization source, Cook *et al.* reported that only protonated alcoholic clusters are observed, and that the protonated $(n-1)$ clusters, $R(OH)_{n-1}H^+$, are generated from neutral n-mers, $(ROH)_n$.[34] Most recently, the possible relationships between the observed ion data and the neutral cluster distributions are discussed for both methanol and ethanol clusters by Shi *et al.* employing the vuv (118 nm) laser ionization.[35]

Most size-selective IR spectroscopic studies of hydrogen-bonded clusters are applied for charged clusters, including $(H_2O)_nH^+$,[3,4] $(NH_3)_nH^+$,[36,37] $(CH_3OH)_nH^+$,[19,38,39] etc. Size-selective measurements are carried out by mass selection using a quadrupole mass filter/octapole ion guide and IR photodissociation. Few IR spectroscopic studies are reported on neutral clusters because (1) the molecular-beam depletion method can achieve size selection, but it is expensive and specifically designed,[10–15] and (2) a size-specific ionization technique by means of an aromatic molecule in mixed clusters is not applicable for pure $(H_2O)_n$, $(NH_3)_n$, and $(CH_3OH)_n$ clusters.[16–18] To the best of our knowledge, only these two techniques are available for studying the spectra of neutral hydrogen-bonded clusters.

In this study, we report the size-specific spectra of methanol clusters, $(CH_3OH)_n$ ($n=4$ to 8), in the OH stretch fundamental region recorded by IR+vuv (118 nm) nonresonant ion-dip (NRIDip-IR) spectroscopy. First, direct correlations between neutral methanol clusters and their corresponding protonated cluster ions are established using 118 nm light as the ionization source. This relation forms the basis for size-selective NRIDip-IR spectroscopy on clusters of specific sizes. That is, population change of $(CH_3OH)_n$ species can be monitored through the $(CH_3OH)_{n-1}H^+$ ion current generated by vuv laser single-photon ionization. Second, IR multiphoton dissociation and subsequent vuv single-photon ionization are utilized as part of the detection chain to achieve size-specific measurements in NRIDip-IR spectroscopy. The correlation of spectral features with cluster size can provide information on hydrogen bonding and cluster geometry with employing this new experimental technique. Additionally, IR+vuv nonresonant ionization detected (NID-IR) spectroscopy is employed to study the OH stretch first overtone of the methanol monomer. The rotational temperature of the clusters is estimated to be at least 50 K based on the monomer rotational envelope. By careful tuning of the vuv ionization wavelength (possible with future development of vuv laser systems), NRIDip-IR and NID-IR spectroscopies may also be applicable to other cluster and noncluster systems.

II. EXPERIMENTAL PROCEDURES

A. Generation and detection of methanol clusters

A molecular beam containing both methanol monomers and clusters is generated by bubbling helium (99.9%, General Air) at a total pressure of 3 atm through a reservoir of spectroscopic grade methanol at room temperature (vapor pressure $\sim$100 torr). The resulting gas mixture of $\sim$5% methanol in helium is then expanded to the vacuum chamber through the face-plate (0.5 mm orifice) of a Parker General Valve Series 9 pulsed solenoid valve. The molecular beam is collimated by a 1.5-mm-diameter skimmer, located around 3 cm downstream from the pulsed nozzle, and then crossed perpendicularly by the vuv (118 nm) laser beam in the ionization region of the time-of-flight mass spectrometer (TOFMS). The counterpropagating IR laser beam is focused upstream from the same jet region by a 40 cm focal length lens.

The generation of the vuv (118 nm) radiation is similar to that used in our metal oxide cluster studies.[32,33] Employing 25 mJ/pulse of 355 nm pump laser light and 200 torr of a 1:10 Xe/Ar mixture, the 118 nm radiation is around 1 μJ/pulse or $\sim$$10^{12}$ photons/pulse. Tunable IR radiation is obtained from an optical parametric oscillator (OPO) (Laser Vision) pumped by an injection-seeded Nd:yttrium aluminum garnet (YAG) laser (Spectra Physics). A type II KDP (KH_2PO_4) doubling crystal is integrated into the OPO laser converting the Nd:YAG laser fundamental output to 532 nm. Two interchangeable sets of nonlinear crystals in the system are used to produce the outputs that provide total coverage from 712 nm to 2.13 μm. For both oscillator configurations, the output beam consists of both signal and idler wavelengths from the down conversion of the 532 nm pump, and a birefringent polarizer (CPBA-10.0, CVI Laser Corp.) is used to separate them. With simple modifications to the optical layout, crystals of the second oscillator can be used to difference-frequency mix the output of the first oscillator with a portion of the 1064 nm pump to provide additional wavelength coverage from 2.89 to 3.3 μm. The OPO laser output between 3000 and 3450 cm^{-1} has a pulse energy of $\sim$15 mJ/pulse and a bandwidth of $\sim$0.4 cm^{-1}. The output between 4760 and 7800 cm^{-1} has a pulsed energy of $\sim$4 mJ/pulse and a bandwidth of $\sim$0.4 cm^{-1}.

The ions created by the vuv laser are extracted by a 250 V potential and accelerated into the time-of-flight (TOF) mass spectrometer at 4 keV of total kinetic energy. Mass-resolved detection is achieved by using a Galileo Electro-Optics multichannel plate (MCP) at the end of a 1.5 m flight tube. In these experiments, the pulsed nozzle and two laser pulses are operated at 10 Hz and synchronized using a digital delay generator (SRS DG535, Stanford Research System). The data acquisition scheme for infrared spectroscopy is similar to that used to record the resonance-enhanced multiphoton ionization (REMPI) spectroscopy described in detail in our previous publications.[40,41]

B. IR+vuv NID-IR spectroscopy

In principle, IR+vuv NID-IR spectroscopy is similar to the IR+UV NID-IR spectroscopy demonstrated by Fujii and

co-workers.[42,43] The vuv (10.5 eV) photon is not energetic enough to ionize a jet-cooled methanol molecule since the ionization energy (IE) of methanol is ~10.84 eV.[44] When the IR laser is scanned to excite jet-cooled methanol monomers to vibrationally excited levels, the total energy of $h\nu_{IR} + h\nu_{vuv}$ is higher than the IE of methanol, and hence vibrationally excited methanol can be ionized by absorption of a 10.5 eV photon. Using this method, the OH stretch first overtone of the methanol monomer is recorded as an increase of the CH_3OH^+ ion signal.

C. IR+vuv NRIDip-IR spectroscopy

NRIDip-IR spectroscopy is developed based on vibrational photodissociation spectroscopy of weakly bound clusters.[45,46] The OPO laser currently used provides spectral coverage between 3000 and 3450 cm^{-1} for $(CH_3OH)_n$ n =4–8 clusters. The OH stretch fundamentals of the neutral monomer, dimer, and trimer are out of this energy range. In NRIDip-IR, the OH stretch fundamental (ν_1) of clustered methanol is excited by IR laser radiation. Since the IR photon energy is larger than the binding energy of neutral methanol clusters, the complex will eventually dissociate depending on the coupling of the molecular modes to the cluster intermolecular degrees of freedom.[15] Under our experimental conditions, photodissociation of $(CH_3OH)_n$ (n=4 to 8) upon excitation of the OH stretch fundamental generates the trimer by loss of (n−3) CH_3OH monomers via a multiphoton process (see Sec. III D). On the other hand, the population change of $(CH_3OH)_n$ clusters can be directly monitored through the intensity change of the $(CH_3OH)_{n-1}H^+$ signal generated by the vuv laser (see Sec. III B). In NRIDip-IR, IR multiphoton dissociation and subsequent vuv single-photon ionization are utilized as part of the detection chain to achieve size-specific measurements (See Sec. III D). The population loss of $(CH_3OH)_n$ (n=4 to 8) clusters upon excitation of the OH stretch vibration is observed as a decrease (dip) in the corresponding $(CH_3OH)_{n-1}H^+$ mass channel signals.

III. RESULTS

A. vuv (118 nm) single-photon ionization of methanol clusters

Figure 1 presents the vuv (118 nm) single-photon ionization/TOFMS spectrum of methanol clusters. Figures 1(b) and 1(c) show expanded structure in the mass regions m/z=28–34 and 63–66, respectively. Assignments of mass peaks are included according to the mass-to-charge (m/z) value. The peak of CH_3OH^+ at m/z=32 in Fig. 1(b) is very weak. It is known that the IE of methanol (10.84 eV) is higher than the vuv photon energy (10.5 eV).[44] Ionization of methanol monomer can occur by two possible mechanisms: (1) sequential absorption of a 118 nm photon followed by a 355 nm photon; or (2) absorption of a 118 nm photon by a CH_3OH that has approximately 3000 cm^{-1} of vibrational energy. Both this mass signal and the one at m/z=31 (CH_2OH^+ or CH_3O^+) are very weak, <0.5% of that observed by 26.5 eV single-photon ionization (by an x-ray laser in this laboratory).[47] The IE of CH_3O is 10.72 eV and the appear-
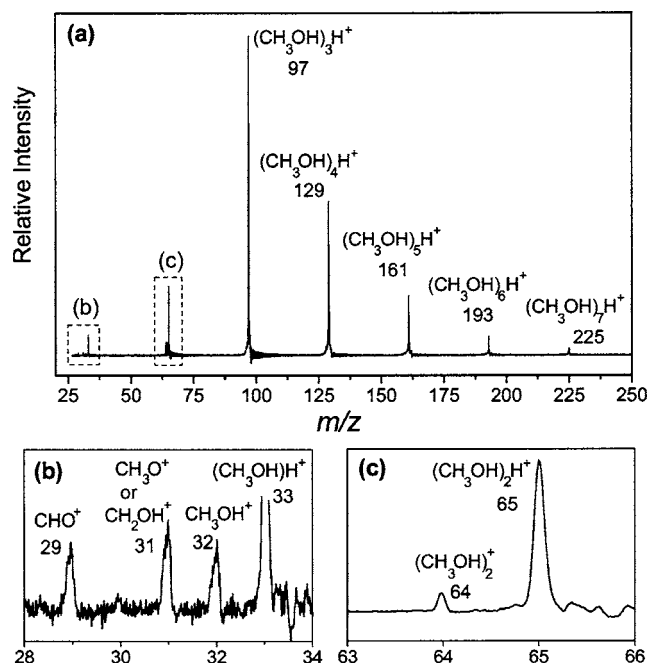

FIG. 1. (a) The vuv single-photon ionization/TOFMS spectra of methanol clusters. (b) and (c) are expanded from (a) in order to show the structure in the mass regions m/z=28–34 and 63–66, respectively.

ance energy for CH_2OH^+ from CH_3OH is 11.65 eV.[48] Thus the multiphoton fragmentation process is suppressed in our experiments as a result of the low vuv photon density ~10^{12} photons/pulse. In Fig. 1(a), the dominant features are a series of strong peaks at m/z=33, 65, 97, 129, 161, 193, and 225, whose masses fit the general formula, $(CH_3OH)_{n-1}H^+$ with n=2–8, except for a peak at m/z=64 [Fig. 1(c)], which is assigned to the parent ion of methanol dimer.

Following the ionization of neutral methanol clusters, a fast proton-transfer reaction of the ionized molecule to neutral partner molecules occurs within the cluster. The protonated methanol cluster ions, $(CH_3OH)_{n-1}H^+$, are generated from neutral clusters, $(CH_3OH)_n$, according to

$$(CH_3OH)_n + h\nu_{vuv} \rightarrow (CH_3OH)_n^+ + e^-, \tag{1a}$$

$$(CH_3OH)_n^+ \rightarrow (CH_3OH)_{n-1}H^+ + CH_3O. \tag{1b}$$

Reaction (1b) has a well-known biomolecular counterpart that proceeds at a near collision rate.[24] One can identify a peak corresponding to methoxy or hydroxymethyl radical at m/z=31 in Fig. 1(b), though it is weak. No additional fragment ions are evident using the 118 nm light as an ionization source. This is in sharp contrast to conventional EI and MPI measurements for which strong fragment congestion in the region of $m/z \leq 200$ is observed.[26–31]

Figure 2 depicts the typical distribution of protonated cluster ions obtained by vuv single-photon ionization. Among them, the strongest peak is due to the protonated trimer. Figure 3 displays the widths of mass peaks for cluster ions. A symmetric peak shape is observed in all cases. The narrowest feature is the peak due to the dimer parent ion $(CH_3OH)_2^+$; its full width at half maximum (FWHM) is 11.4 ns, almost equal to the width of vuv laser pulse. In the se-
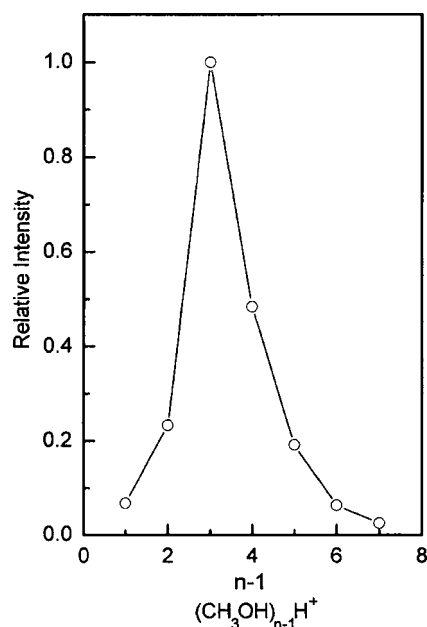
FIG. 2. Distribution of protonated cluster ions, $(CH_3OH)_{n-1}H^+$ for $n=2$ to 8, normalized according to the intensity of $(CH_3OH)_3H^+$.

quence of $(CH_3OH)_{n-1}H^+$ ($n=2$–6) peaks, the mass peak width increases with increasing the cluster size. The FWHM values of $(CH_3OH)_{n-1}H^+$ features for $n=2$–6 are 14.0, 15.6, 17.4, 19.4, and 20.0 ns, respectively. The widths of $n=7$ and 8 peaks (not shown in Fig. 3) are almost the same as that of the $n=6$ peak.

B. Thermodynamics and fragmentation probability of $(CH_3OH)_{n-1}H^+$

Does the observed distribution of protonated cluster ions, generated via the proton transfer reaction (1b) following vuv single-photon ionization (1a), represent the neutral
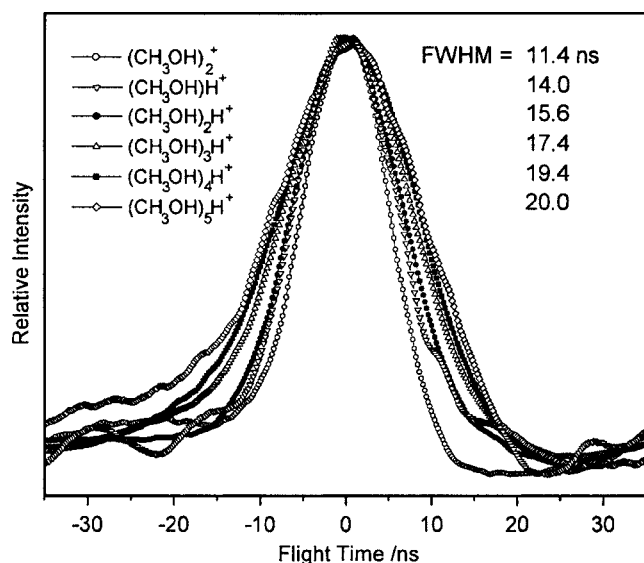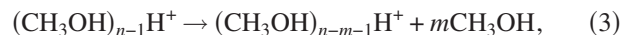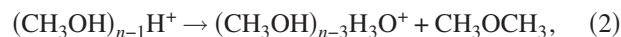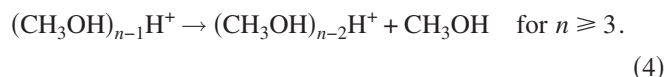

FIG. 3. The peak width of ionic clusters obtained by vuv single-photon ionization.

cluster distribution? If only reaction (1) occurs, the answer is yes; however, the freshly generated $(CH_3OH)_{n-1}H^+$ clusters may further dissociate according to reactions

$$(CH_3OH)_{n-1}H^+ \rightarrow (CH_3OH)_{n-3}H_3O^+ + CH_3OCH_3, \quad (2)$$

$$(CH_3OH)_{n-1}H^+ \rightarrow (CH_3OH)_{n-m-1}H^+ + mCH_3OH, \quad (3)$$

depending on the excess energy released into the protonated cluster ions during the ionization/proton transfer reaction processes. The production of $(CH_3OH)_{n-3}H_3O^+$ via reaction (2) is observed in conventional EI and MPI experiments,[26–31] but this is not the case in the present study using 118 nm light as the ionization source. No mass peaks can be assigned to $(CH_3OH)_{n-3}H_3O^+$ in Fig. 1(a).

Protonated cluster ions may also undergo unimolecular dissociation as shown in reaction (3)—the evaporative loss of neutral monomer units from protonated cluster ions. The endothermic evaporation process consumes the excess energy released into a protonated cluster ion and freezes the cluster ion into a more ordered structure.[49] Reaction (3) is a relatively slow process.[31] For linear TOFMS (no reflectron), dissociation products born in the drift tube (field-free flight region) appear at the same masses as the parent ions, such that the distribution of parent ions will not be distorted. On the other hand, one can estimate the dissociation probability for the simplest case of reaction (3) in the acceleration region, i.e., $(CH_3OH)_{n-1}H^+$ losing one monomer,

$$(CH_3OH)_{n-1}H^+ \rightarrow (CH_3OH)_{n-2}H^+ + CH_3OH \quad \text{for } n \geqslant 3.$$
$$(4)$$

Employing Rice-Ramsperger-Kassel (RRK) theory, the rate constant for dissociation (k_{n-1}) and the fraction of cluster ions undergoing dissociation (N_f) are estimated as

$$k_{n-1} = \nu(1 - E_{n-1,\text{dis}}/E_{n-1,\text{exc}})^{S-1}, \quad (5)$$

$$N_f = N_0(1 - e^{-kt}). \quad (6)$$

The dissociation energy for $(CH_3OH)_{n-1}H^+$ losing one monomer, $E_{n-1,\text{dis}}$, is available based on published thermodynamic results.[50] $E_{n-1,\text{exc}}$ is the excess energy deposited into $(CH_3OH)_{n-1}H^+$ during the 118 nm single-photon ionization process, which can be calculated utilizing the Born-Haber cycles given in Fig. 4. A value of $\nu=10^{13}$ s^{-1} is taken for the vibrational frequency of the dissociation reaction coordinate. S is the number of oscillators in the $(CH_3OH)_{n-1}H^+$ cluster that contributes to reaction (4). The residence time of $(CH_3OH)_{n-1}H^+$ clusters in the acceleration region of the TOFMS, t, is ~ 1.5 μs. N_0 and N_f are the initial number of cluster ions and the number of fragment ions, respectively. N_f/N_0 gives the probability for $(CH_3OH)_{n-1}H^+$ losing one monomer.

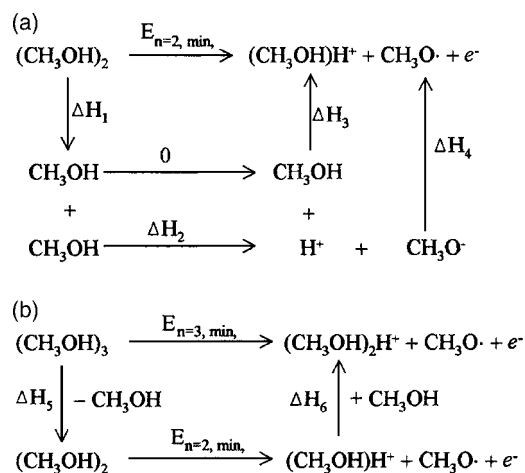FIG. 4. Born-Haber cycles utilized to calculate the minimum energy to activate the reaction from $(CH_3OH)_n$ to $(CH_3OH)_{n-1}H^+ + CH_3O\cdot + e^-$, $E_{n,min}$, for $n=2$ (a) and $n=3-8$ (b). See text for details.

The energy difference between the reactants, e.g., $(CH_3OH)_2$, and the products, e.g., $(CH_3OH)H^+ + CH_3O\cdot + e^-$, can be calculated using the Born-Haber cycle shown in Fig. 4(a). This is the minimum energy required to activate a reaction from $(CH_3OH)_n$ to $(CH_3OH)_{n-1}H^+ + CH_3O\cdot + e^-$, $n=2$, and it is denoted as $E_{n=2,min}$. Using the values [see Fig. 4(a)], $\Delta H_1 = -$(binding energy of neutral dimer, $E_{n=2,b}) = 0.278$ eV (obtained from theoretical calculations),[14,15] $\Delta H_2 = 1596.4$ kJ/mol $= 16.546$ eV,[48] ΔH_3 = the proton affinity of $CH_3OH = -754.3$ kJ/mol $= -7.818$ eV,[48] $\Delta H_4 = -$(electron affinity of $OH\cdot) = 1.572$ eV,[51] one can calculate $E_{n=2,min} = \Delta H_1 + \Delta H_2 + \Delta H_3 + \Delta H_4 = 10.578$ eV. Using the cycle (b) of Fig. 4, one can calculate the $E_{n=3,min} = \Delta H_5 + E_{n=2,min} + \Delta H_6 = 9.56$ eV, using $\Delta H_5 = (E_{n=2,b} - E_{n=3,b}) = 0.416$ eV, ΔH_6 is the energy for adding a monomer to $(CH_3OH)H^+ = -E_{n-1=2,dis} = -1.435$ eV. In the same way $E_{n,min}$ are calculated for $n=4$ to 8.

In the present study, a 10.5 eV photon is employed to initiate the reaction from $(CH_3OH)_n$ to $(CH_3OH)_{n-1}H^+ + CH_3O\cdot + e^-$. The energy emitted by reaction (1) is $\Delta H_n = E_{n,min} - 10.5$ eV. The $\Delta H_{n=2} = 0.08$ eV indicates that 10.5 eV is just near the threshold of the IE of $(CH_3OH)_2$ cluster. Comparison of the mass spectra of methanol clusters obtained at single photon 10.5 eV and at 26.5 eV ionization by linear TOFMS (in different apparatuses) suggests that energy removed by the ionized electron is roughly equal to vuv photon energy—IE_n [the vertical IE of $(CH_3OH)_n$ clusters].[47] Since 10.5 eV is near the threshold of IE_n, neglecting the energy removed by the ionized electron is reasonable in the present study for 10.5 eV ionization process. Neglecting translational-energy release, $E_{n-1,exc} = -\Delta H_n$ is the maximum excess energy deposited in the $(CH_3OH)_{n-1}H^+$ cluster by reaction (1a) due to 10.5 eV photon.

The unknown parameter in Eqs. (5) and (6) is the S. If only the number of van der Waals modes of the $(CH_3OH)_{n-1}H^+$ cluster, $S = 6n-9$,[52] is considered, N_f/N_0 is calculated $> 99\%$ for $n \geqslant 5$. This is clearly not correct because $(CH_3OH)_{n-1}H^+$ $n=5-8$ clusters are experimentally observed. If the number of total molecular modes of the $(CH_3OH)_{n-1}H^+$ cluster, $S = 18n-21$,[53] is used, N_f/N_0 is calculated to be ≈ 0. Results of single-photon 26.5 eV ionization and reflection TOFMS detection for the $(CH_3OH)_{n-1}H^+$ cluster[47] suggest that S is roughly equal to the number of van der Waals modes $+3$ molecular modes for each CH_3OH molecule in the cluster, i.e., $S = (6n-9) + 3(n-1) = 9n-12$. Table I presents the values of $E_{n,b}$, $E_{n-1,dis}$, $E_{n,min}$, $E_{n-1,exc}$, S_{n-1}, and k_{n-1} for $2 \leqslant n \leqslant 8$. Equation (6) yields a $N_f/N_0 < 8\%$ for $n=3-8$ $(CH_3OH)_{n-1}H^+$ clusters. Based on the above experimental and calculational results, we conclude that the detected distribution of protonated cluster ions basically correlates to the distribution of neutral clusters for linear TOFMS if 118 nm light is employed as the ionization source.

As a fragmented ion from reaction (1), $(CH_3OH)_{n-1}H^+$ exhibits a broad mass peak with the FWHM larger than the FWHM of the vuv laser pulse (Fig. 3). The calculated ΔH_n in Table I indicates that reaction (1) is progressively more exothermic with increasing n of $(CH_3OH)_n$ at a fixed 118 nm ionization wavelength. Note that ΔH_n is obtained based on thermodynamic calculations, which do not involve the actual mechanism, i.e., vuv single-photon ionization (1a) followed by the proton transfer reaction (1b). For $(CH_3OH)_n$ clusters,

TABLE I. Parameters used in calculating the dissociation probability for $(CH_3OH)_{n-1}H^+$ losing one monomer within the acceleration region of TOF mass spectrometer.

n	2	3	4	5	6	7	8
$E_{n,b}$ (eV)[a]	−0.278	−0.694	−1.368	−1.935	−2.467	−2.909	−3.377
E_{n-1},dis (eV)[b]		1.435	1.140	0.698	0.585	0.542	0.516
$E_{n,min}$ (eV)[c]	10.578	9.56	9.09	8.96	8.91	8.81	8.76
$E_{n-1,exc}$ (eV)[d] $-\Delta H_n$ (eV)[e]	−0.08	0.94	1.41	1.54	1.59	1.69	1.74
S_{n-1}[f]		15	24	33	42	51	60
k_{n-1} (s^{-1})[g]		0	3×10^{-4}	4×10^4	6×10^4	4×10^4	1×10^4

[a]$E_{n,b}$, the binding energy of $(CH_3OH)_n$, from Ref. 14.
[b]$E_{n-1,dis}$, the dissociation energy for $(CH_3OH)_{n-1}H^+ \rightarrow (CH_3OH)_{n-2}H^+ + CH_3OH$, from Ref. 50.
[c]$E_{n,min}$, the minimum energy to initiate the reaction from $(CH_3OH)_n$ to $((CH_3OH)_{n-1}H^+ + CH_3O\cdot + e^-)$, calculated from the Born-Haber cycles displayed in Fig. 4.
[d]$E_{n-1,exc} = -\Delta H_n$, the maximum energy that can be deposited into $(CH_3OH)_{n-1}H^+$.
[e]ΔH_n, energy emitted by reaction (1).
[f]See Sec. III B for a discussion of the value of S_{n-1}.
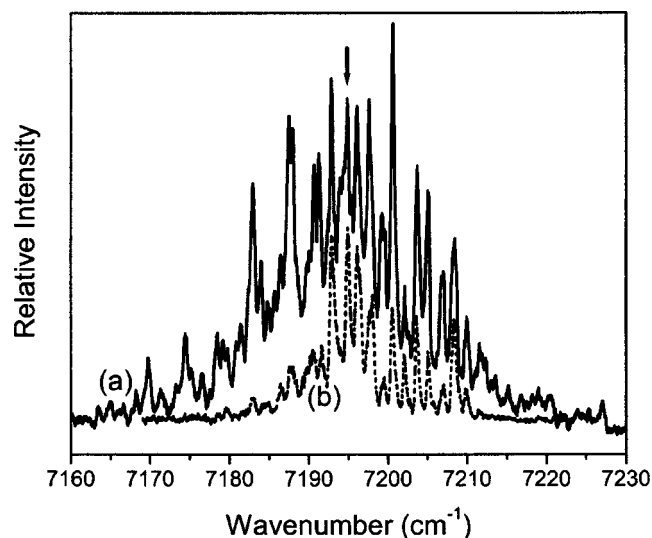[g]k_{n-1}, the reaction rate for $(CH_3OH)_{n-1}H^+ \rightarrow (CH_3OH)_{n-2}H^+ + CH_3OH$, calculated by RRK theory.

FIG. 5. The OH stretch first overtone vibration of jet-cooled methanol momomer recorded by NID-IR spectroscopy using (a) ~5% methanol vapor seeded in 3 atm of helium and (b) 0.5% methanol premixed with helium at 3 atm. The arrow indicates the IR laser frequency used in recording the mass spectra displayed in Fig. 6.

the increase in ΔH_n with increasing n from 2 to 8 includes both the decrease in IE and the increase in proton affinity.

C. IR+vuv (118 nm) NID-IR spectroscopy of methanol monomer in the OH stretch first overtone region

Rizzo and co-workers found large torsion-rotation couplings in the OH stretch overtone vibrations of methanol, employing laser-assisted photofragment spectroscopy (IRLAPS).[54,55] Here we present a simple excitation scheme, IR+vuv NID-IR spectroscopy, to record the OH stretch first overtone vibration of jet-cooled methanol (Fig. 5). For non-resonant IR radiation, the CH_3OH^+ signal generated by the vuv laser is small (<5 mV). With the IR laser-frequency fixed at 7194.5 cm^{-1} (marked by the arrow in Fig. 5), the total energy of $h\nu_{IR}+h\nu_{vuv}$ is ~11.4 eV, higher than the IE for methanol (10.84 eV). As shown in Fig. 6, the CH_3OH^+ intensity in the presence of IR radiation at 7194.5 cm^{-1}
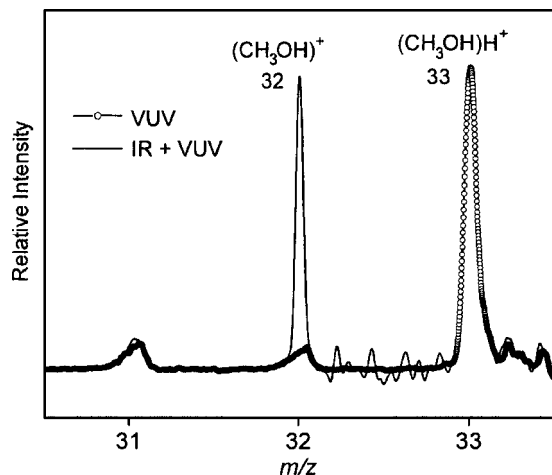

FIG. 6. The mass spectra in the region of $m/z=31–33$ in the absence (open circle) and presence (solid line) of IR radiation at 7194.5 cm^{-1} resonant with the OH stretch first overtone vibration of methanol monomer.

(solid line) is almost ten times that in the absence of IR radiation (open circle), while the intensities in mass channels 29 and 33 remain constant. Scanning the IR laser through this resonance range, the OH stretch first overtone spectrum of jet-cooled methanol is obtained as an increase in the CH_3OH^+ intensity. The additional energy in the molecule from $h\nu_{IR}+h\nu_{vuv}$ excitation is sufficient to ionize the methanol monomer. The increase in ionization efficiency for the IR+vuv NID-IR scheme can result from large Franck-Condon factors between the vibrationally excited states of the neutral and vibronic combination levels of the cation.[56]

In Fig. 5, spectrum (a) is taken under clustering conditions by expanding a gas mixture of methanol vapor seeded in helium. The concentration of methanol in the gas mixture is ~5% for a typical carrier gas (He) pressure of 3 atm. Under these conditions cluster mass channel signals are not observed to change in intensity (±5%) with the IR laser tuned to a OH stretch overtone resonance. This implies that Fig. 5(a) does not arise from fragmented CH_3OH. Spectrum (b) is recorded using 0.5% methanol premixed with helium at 3 atm. The cluster signal intensity under conditions to record spectrum (b) is reduced by a factor of ~100 from that under clustering conditions. Employing the rotational constants determined by Rueda et al.,[54] rotational envelope simulation is achieved without consideration of the torsion-rotation coupling, providing a rotational temperature T_{rot} ~50 and 10 K for spectra (a) and (b), respectively. This indicates that the adiabatic expansion promotes the formation of methanol clusters. The heat of formation of clusters has an effect on the supersonic cooling, leading to a high T_{rot} for the spectrum recorded under clustering conditions and helium cooling.

D. IR+vuv (118 nm) NRIDip-IR spectroscopy of methanol clusters in the OH stretch fundamental region

We emphasize in Sec. III B that the detected distribution of protonated cluster ions directly correlates with the distribution of neutral clusters if 118 nm light is employed as the ionization source. That is, the population change of $(CH_3OH)_n$ clusters can be directly monitored through the intensity change of the $(CH_3OH)_{n-1}H^+$ signal generated by the vuv laser.

Figure 7 presents a survey of the intensity changes in different mass channels upon irradiating the cluster molecular beam with the IR laser beam at 3230 cm^{-1}. The $(CH_3OH)_n$ ($n=1–4$) species do not absorb at this energy.[22,23] By comparing spectrum (b) with (a), a clear decrease upon IR irradiation of the cluster beam is observed for the mass peaks of $(CH_3OH)_{n-1}H^+$ $n=5$ to 8, while the $(CH_3OH)_3H^+$ peak remains almost the same. Moreover, an intensity increase in the $(CH_3OH)_2H^+$ and $(CH_3OH)^+$ mass channels is quite evident and large, a factor of 5 for $(CH_3OH)_2H^+$ and a factor of 10 for $(CH_3OH)^+$. Intensity decrease in the mass channels of $(CH_3OH)_{n-1}H^+$ $n=5$ to 8 results from the population loss of neutral $n=5$ to 8 $(CH_3OH)_n$ clusters upon IR absorption at 3230 cm^{-1}. Meanwhile, the population increase of the neutral trimer [generating $(CH_3OH)_2H^+$ upon ionization] and monomer is revealed by the intensity increase of
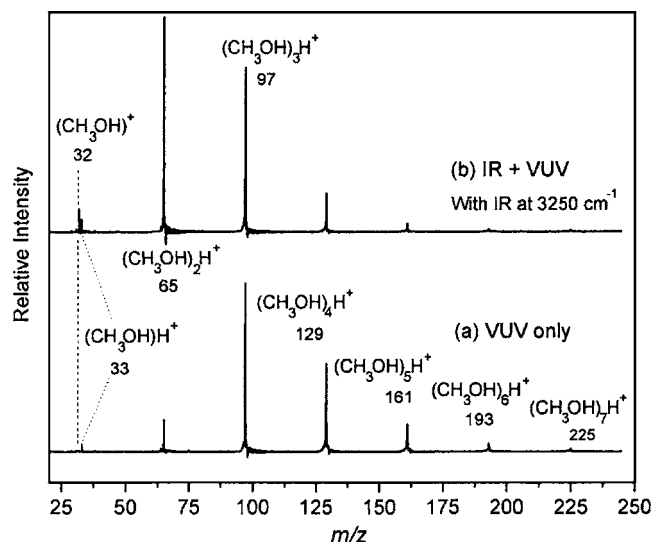
FIG. 7. The mass spectra of methanol clusters in the absence (a) and presence (b) of IR radiation at 3230 cm^{-1}. The IR laser frequency at 3230 cm^{-1} falls in the range of the OH stretch fundamental of $(CH_3OH)_n$ for $n=5-8$, and out of range for $n=4$.

$(CH_3OH)_2H^+$ and $(CH_3OH)^+$ signals. Therefore, neutral $(CH_3OH)_n$ clusters for $n=5$ to 8 are fragmented into the trimer by loss of $(n-3)$ monomers upon IR excitation at 3230 cm^{-1}. If the IR laser is fixed at 3350 cm^{-1}, an increase of the $(CH_3OH)_2H^+$ and $(CH_3OH)^+$ signals is also observed, accompanied by a decrease of the $(CH_3OH)_3H^+$ intensity. Note that at 3350 cm^{-1} the $(CH_3OH)_n$ $n=4-8$ species absorb and $n=1-3$ species do not absorb.[15,22,23] Therefore, IR photodissociation of the neutral tetramer also produces the trimer by loss of one monomer. The IR laser pulse energy used in recording the Fig. 7 spectrum is ~12 mJ/pulse. A plot of the IR laser power versus the mass spectral feature intensity yields a photon number dependence of 1.3 to 1.5 photon/unit of signal intensity, thus the IR photodissociation of neutral methanol clusters at the OH stretch fundamental is a multiphoton process with saturation under our experimental conditions,

$$(CH_3OH)_n + xh\nu_{IR} \rightarrow (CH_3OH)_3$$
$$+ (n-3)CH_3OH \quad \text{for } n=4 \text{ to } 8.$$

$$(7)$$
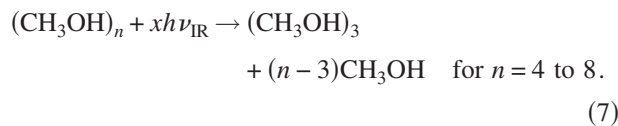
The CH_3OH produced in reaction (7) has at least ~3000 cm^{-1} energy obtained from the IR multiphoton dissociation of neutral methanol clusters, and thus can be ionized directly by the vuv laser.

The size-specific detection chain in NRIDip-IR spectroscopy consists of two parts. First, $(CH_3OH)_n$ clusters for $n \geq 4$ dissociate mainly into $(CH_3OH)_3$ by loss of $(n-3)$ monomers (see Fig. 7) upon IR multiphoton absorption under our experimental conditions [reaction (7)]. Therefore, distortion of the NRIDip-IR spectrum arising from production of $(CH_3OH)_k$ from the fragmentation of larger clusters $(CH_3OH)_m$ $(m>k \geq 4)$ is minimized. Second, the population loss of $(CH_3OH)_k$ owing to IR photodissociation can be monitored through the $(CH_3OH)_{k-1}H^+$ ion current generated by the vuv laser. If IR radiation is not resonant with the OH
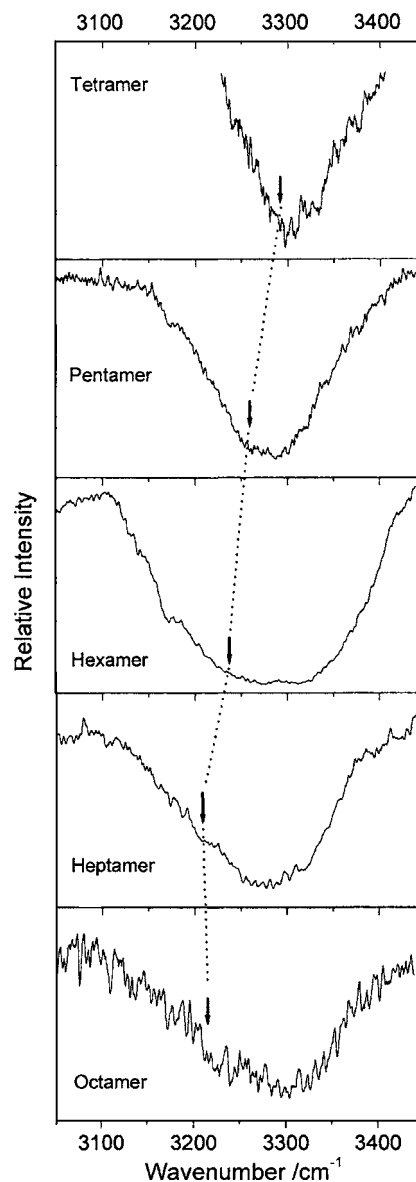

FIG. 8. The OH stretch fundamental vibration of methanol clusters, $(CH_3OH)_n$, for $n=4$ (top) to 8 (bottom), recorded by NRIDip-IR spectroscopy through monitoring the $(CH_3OH)_{n-1}H^+$ signal generated by vuv laser ionization. The solid arrow indicates the lowest-energy peak contributed to each cluster spectrum, which is obtained by the Lorentzian multiple-peak fitting.

stretch vibration of $(CH_3OH)_k$, the $(CH_3OH)_{k-1}H^+$ intensity generated by the vuv laser remains constant. In NRIDip-IR spectroscopy, the population loss of $(CH_3OH)_k$ induced by the IR multiphoton absorption in the OH stretch (ν_1) fundamental region is recorded as a decrease (dip) of the $(CH_3OH)_{k-1}H^+$ intensity.

Figure 8 plots the intensity change of $(CH_3OH)_{n-1}H^+$ from $n=4$ (top trace) to 8 (bottom trace) by scanning the IR laser frequency, corresponding to the OH stretch vibration spectra of $(CH_3OH)_n$ for $n=4$ to 8. The absorbance of the neutral tetramer at 3230 cm^{-1} is small. This is why the $(CH_3OH)_3H^+$ peak remains almost the same in Fig. 8 upon irradiating the cluster beam with the IR laser beam at 3230 cm^{-1}. Cluster spectra in Fig. 8 show large redshifts as compared with the free OH stretch at 3681.5 cm^{-1} for methanol monomer. Based on a curve fitting spectral deconvolu-

TABLE II. Frequencies of the fitted Lorentzian curves for spectra of $(CH_3OH)_n$, $n=4$ to 8, after excitation of the ν_1 mode. Values in the parentheses are from Refs. 13 and 15.

$n=4$[a]	3289 (3270)	3329 (3335)	
$n=5$[b]	3249 (3240)	3302 (3300)	3349 (3340)
$n=6$[a]	3234 (3230)	3338 (3320)	
$n=7$[b]	3207 (3210)	3270 (3280)	3325 (3320, 3255, 3410)
$n=8$[a]	3232 (3220, 3241)	3315 (3380)	

[a]The values in the parentheses are directly reported in Refs. 13 and 15.
[b]The values in the parentheses are read from the spectra in Refs. 13 and 15.

tion program (ORIGIN 6.0, see below), the even-sized methanol clusters, including the tetramer, hexamer, and octamer, present structured spectra with two resolvable peaks. In the case of the odd-sized methanol clusters, the heptamer exhibits a three-peak resolved spectrum, while only one well-resolved peak is observed for the pentamer.

IV. DISCUSSION

Huisken et al.[10,11] and Buck et al.[12–15] report IR spectral results based on size-selected detection of methanol clusters, employing molecular-beam depletion combined IR photodissociation spectroscopy. Based on the calculated minimum-energy configurations of the cluster structures, these authors also develop a perturbation approach to reproduce the general structures of the spectra for $n=4$ to 9 $(CH_3OH)_n$ clusters.[12,14,15] The NRIDip-IR spectra in Fig. 8 are essentially in agreement with the results reported in Refs. 10–15. To analyze these cluster spectra in detail, Lorentzian multiple-peak fittings are conducted by using ORIGIN 6.0 software. Two-peak Lorentzian fitting is adopted for the even-sized cluster spectra, while three-peak Lorentzian fitting is employed for the spectra of heptamer and pentamer. Maxima of the fitted Lorentzian peaks are given in Table II as a function of cluster size. Values reported by Buck and Ettischer[13] are also included in parentheses for comparison. Our values are consistent with those obtained by Buck and Ettischer.[13] The solid arrow in each spectrum presented in Fig. 8 indicates the lowest-energy feature contributed to the spectrum, according to the resolved Lorentzian peak fitting. This lowest-energy component is redshifted with increasing cluster size as shown by the dashed vertical line between spectra. This depicts the development of hydrogen bonding in methanol clusters as a function of cluster size. Positions of the lowest energy peak in the heptamer and octamer spectra finally converge to ~ 3220 cm^{-1}, which is close to the OH stretch value measured for solid methanol.[22,57]

The double-peak structures observed for the IR spectra of even-sized methanol clusters with $n=4$, 6, and 8 can be related to their calculated lowest-energy conformations: rings of S_n symmetry with the methyl group pointing alternatively up and down.[13–15] Calculations show that the two peaks derive from the coupled symmetric and antisymmetric motion of all the stretching oscillators. Lorentzian peak positions fitted to the spectra of the tetramer and hexamer (Table II) are qualitatively consistent with those reported by Buck et al.[13,15] An additional folded ring isomer of the octamer with S_4 symmetry is reported in the crossed beam

studies,[13,15] but is not well resolved in the present study. The odd-number methanol clusters are cyclic with no special symmetry, since the additional methyl group cannot be placed in any symmetric way. This gives at most, depending somewhat on the IR-transition moments, five bands for the pentamer, and seven bands for the heptamer. Again, fitted Lorentzian peaks for the pentamer and heptamer spectra in Table II correspond very well to major peaks reported by Buck et al.;[13,15] however, some minor peaks are not observed in the present study.

Huisken et al. and Buck et al. utilized the molecular-beam depletion technique to separate methanol clusters by scattering with helium atoms in a specifically designed crossed-beam arrangement.[10–15] In our experiments, all clusters are mixed together in the molecular beam. Size-specific detection is achieved through the IR multiphoton dissociation and vuv (10.5 eV) single-photon ionization detection chain. The IR+vuv NRIDip-IR spectroscopy described in the present study may also be applicable to other neutral cluster systems. The prerequisites are (1) that vuv photon energy $\geqslant$ IE of the clusters of interest, and (2) that neutral cluster distribution can be obtained using vuv single-photon ionization, that is, intensity of the monitored ionic species generated by the vuv laser should be determined by the population of its neutral parent. Application of NID-IR spectroscopy to other noncluster systems is also possible, if $h\nu_{vuv} <$ IE of the system $\leqslant h\nu_{IR} + h\nu_{vuv}$. In any event, the vuv wavelength may need to be tuned depending on the systems studied.

Since the OH stretch first overtone spectrum of the methanol monomer in Fig. 5(a) is recorded under clustering conditions, one might initially assume that $T_{rot} \sim 50$ K for Fig. 5(a) can also be estimated for clusters; however, the heat of formation of clusters formed in the adiabatic expansion and the internal energy of clusters (especially larger sizes) formed above the methanol vapor may raise T_{rot}, even though the collision cross section with helium atoms is larger for clusters than for the monomer. $T_{rot} \sim 50$ K as the lower limit for clusters in the beam is a more reasonable estimate.

V. CONCLUSION

Small methanol clusters are detected using vuv (118 nm) single-photon ionization/TOF mass spectrometer in the supersonic expansion. The protonated cluster ions, produced through proton-transfer reactions following the vuv single-photon ionization, essentially correlate to the neutral clusters. There is not enough excess energy released into the protonated cluster ions to initiate further fragmentation within the 1.5 μs time frame for detection of such processes. Clusters of $(CH_3OH)_n$ for $n=4$ to 8 are found to dissociate mainly into the trimer by loss of $(n-3)$ monomers upon the IR multiphoton absorption in the OH stretch fundamental region. Employing IR photodissociation and vuv single-photon ionization as part of the cluster detection chain, size-specific spectra of $(CH_3OH)_n$ for $n=4$ to 8 are recorded using IR +vuv (118 nm) NRIDip-IR spectroscopy by monitoring the $(CH_3OH)_{n-1}H^+$ mass channel signal. The general structures and gross features of cluster spectra are consistent with previous theoretical calculations. The lowest-energy peak con-

tributed to each cluster spectrum is redshifted with increasing the cluster size ($n=4$ to 8), and converges to ~ 3220 cm^{-1} in the heptamer and octamer, close to the OH stretch value measured for solid methanol. The rotational temperature for the monomer is estimated to be ~ 50 K based on simulation of the OH stretch first overtone spectrum of the jet-cooled methanol monomer, recorded by IR +vuv (118 nm) NID-IR spectroscopy.

ACKNOWLEDGMENTS

[1] G. A. Jeffrey, *An Introduction to Hydrogen Bonding* (Oxford University Press, New York, 1997).

[2] S. Scheiner, *Hydrogen Bonding: A Theoretical Perspective* (Oxford University Press, New York, 1997).

[3] M. Miyazaki, A. Fujii, T. Ebata, and N. Mikami, Science **304**, 1134 (2004).

[4] J. W. Shin, N. I. Hammer, E. G. Diken, M. A. Johnson, R. S. Walters, T. D. Jaeger, M. A. Duncan, R. A. Christie, and K. D. Jordan, Science **304**, 1137 (2004).

[5] B. H. Torrie, S. X. Weng, and B. M. Powell, Mol. Phys. **67**, 575 (1989).

[6] T. Yamaguchi, K. Hidaka, and A. K. Soper, Mol. Phys. **97**, 603 (1999).

[7] S. Sarkar and R. N. Joarder, J. Chem. Phys. **99**, 2032 (1993).

[8] A. Arencibia, M. Taravillo, F. J. Perez, J. Nunez, and V. G. Baonza, Phys. Rev. Lett. **89**, 195504 (2002).

[9] A. H. Narten and A. Habenschuss, J. Chem. Phys. **80**, 3387 (1984).

[10] F. Huisken, A. Kulcke, C. Laush, and J. M. Lisy, J. Chem. Phys. **95**, 3924 (1991).

[11] F. Huisken, M. Kaloudis, M. Koch, and O. Werhahn, J. Chem. Phys. **105**, 8965 (1996).

[12] U. Buck and B. Schmidt, J. Chem. Phys. **98**, 9410 (1993).

[13] U. Buck and I. Ettischer, J. Chem. Phys. **108**, 33 (1998); **100**, 6974 (1994).

[14] U. Buck, J. G. Siebers, and R. J. Wheatley, J. Chem. Phys. **108**, 20 (1998).

[15] U. Buck and F. Huisken, Chem. Rev. (Washington, D.C.) **100**, 3863 (2000).

[16] R. N. Pribble, F. C. Hagemeister, and T. S. Zwier, J. Chem. Phys. **106**, 2145 (1997).

[17] F. C. Hagemeister, C. J. Gruenloh, and T. S. Zwier, J. Phys. Chem. A **102**, 82 (1998).

[18] T. S. Zwier, Annu. Rev. Phys. Chem. **47**, 205 (1996).

[19] A. Fujii, S. Enomoto, M. Miyazaki, and N. Mikami, J. Phys. Chem. A **109**, 138 (2005).

[20] S. Coussan, A. Loutellier, J. P. Perchard, S. Racine, A. Peremans, A. Tadjeddine, and W. Q. Zheng, J. Chem. Phys. **107**, 6526 (1997).

[21] S. Coussan, Y. Bouteiller, A. Loutellier, J. P. Perchard, S. Racine, A. Peremans, W. Q. Zheng, and A. Tadjeddine, Chem. Phys. **219**, 221 (1997).

[22] R. A. Provencal, J. B. Paul, K. Roth, C. Chapo, R. N. Casaes, R. J. Saykally, G. S. Tschumper, and H. F. Schaefer, III, J. Chem. Phys. **110**, 4258 (1999).

[23] T. Haber, U. Schmitt, and M. Suhm, Phys. Chem. Chem. Phys. **1**, 5573 (1999).

[24] M. T. Bowers, T. Su, and V. G. Anicich, J. Chem. Phys. **58**, 5175 (1973).

[25] L. M. Bass, R. D. Cates, M. F. Jarrold, N. J. Kirchner, and M. T. Bowers, J. Am. Chem. Soc. **105**, 7024 (1983).

[26] L. W. Sieck, F. P. Abramson, and J. H. Futrell, J. Chem. Phys. **45**, 2859 (1966).

[27] A. K. Shukla and A. J. Stace, J. Phys. Chem. **92**, 2579 (1988).

[28] M. S. El-Shall, C. Marks, L. W. Sieck, and M. Meot-Ner (Mautner), J. Phys. Chem. **96**, 2045 (1992).

[29] S. Morgan and A. W. Castleman, Jr., J. Am. Chem. Soc. **109**, 2867 (1987).

[30] S. Morgan, R. G. Keesee, and A. W. Castleman, Jr., J. Am. Chem. Soc. **111**, 3841 (1989).

[31] S. Morgan and A. W. Castleman, Jr., J. Phys. Chem. **93**, 4544 (1989).

[32] D. N. Shin, Y. Matsuda, and E. R. Bernstein, J. Chem. Phys. **120**, 4150 (2004).

[33] Y. Matsuda and E. R. Bernstein, J. Phys. Chem. A **109**, 3803 (2005).

[34] K. D. Cook, G. G. Jones, and J. W. Taylor, Int. J. Mass Spectrom. Ion Phys. **35**, 273 (1980).

[35] Y. J. Shi, S. Consta, A. K. Das, B. Mallik, D. Lacey, and R. H. Lipson, J. Chem. Phys. **116**, 6990 (2002).

[36] J. M. Price, M. W. Crofton, and Y. T. Lee, J. Chem. Phys. **91**, 2749 (1989).

[37] J. M. Price, M. W. Crofton, and Y. T. Lee, J. Phys. Chem. **95**, 2182 (1991).

[38] H. C. Chang, J. C. Jiang, S. H. Lin, Y. T. Lee, and H. C. Chang, J. Phys. Chem. A **103**, 2941 (1999).

[39] X. Zang, X. Yang, and A. W. Castleman, Jr., Chem. Phys. Lett. **185**, 298 (1991).

[40] R. Disselkamp and E. R. Bernstein, J. Chem. Phys. **98**, 4339 (1993).

[41] E. R. Bernstein, K. Law, and M. Schauer, J. Chem. Phys. **80**, 207 (1984).

[42] T. Omi, H. Shitomi, N. Sekiya, K. Takazawa, and M. Fujii, Chem. Phys. Lett. **252**, 287 (1996).

[43] S. Ishiuchi, H. Shitomi, H. K. Takazawa, and M. Fujii, Chem. Phys. Lett. **283**, 243 (1998).

[44] W. Tao, R. B. Klemn, F. L. Nesbitt, and L. J. Stief, J. Phys. Chem. **96**, 104 (1992).

[45] R. E. Miller, Science **240**, 447 (1988).

[46] R. E. Miller, J. Phys. Chem. **90**, 3301 (1986).

[47] F. Dong, S. Heinbuch, J. J. Rocca, and E. R. Bernstein (in preparation). Briefly, with consideration of the difference in ionization cross sections at 26.5 and 10.5 eV, the distribution of protonated methanol clusters detected by 26.5 eV single-photon ionization/linear TOFMS is quite similar to that obtained in the present study. Results of 26.5 eV single photon ionization/reflectron TOFMS reveal that reaction (4) occurs only for $n \geqslant 6$ $(CH_3OH)_{n-1}H^+$ clusters.

[48] The NIST Chemistry Webbook, http://webbook.nist.gov/chemistry.

[49] C. E. Klots, J. Chem. Phys. **83**, 5854 (1985).

[50] E. P. Grimsrud and P. Kebarle, J. Am. Chem. Soc. **95**, 7939 (1973).

[51] T. M. Ramond, G. E. Davico, and R. L. Schwartz, J. Chem. Phys. **112**, 1158 (2000).

[52] van der Waals modes of $(CH_3OH)_{n-1}H^+$ cluster, $S=6n-9$, is obtained by contribution from $(n-1)$ CH_3OH molecules, $6(n-1)-6$, plus three degrees of freedom from the proton.

[53] Molecular modes of $(CH_3OH)_{n-1}H^+$ cluster, $S=18n-21$, is obtained according to $S=3N-6$, and $N=6(n-1)+1$ is the number of atoms in the $(CH_3OH)_{n-1}H^+$ cluster.

[54] D. Rueda, O. V. Boyarkin, T. R. Rizzo, I. Mukhopadhyay, and D. S. Perry, J. Chem. Phys. **116**, 91 (2002).

[55] D. Rueda, O. V. Boyarkin, T. R. Rizzo, A. Chirokolava, and D. S. Perry, J. Chem. Phys. **116**, 91 (2002).

[56] X. M. Qian, A. H. Kung, T. Zhang, K. C. Lau, and C. Y. Ng, Phys. Rev. Lett. **91**, 233001 (1993).

[57] S. Coussan, Y. Bouteiller, A. Loutellier, J. P. Perchard, S. Racine, A. Peremans, W. Q. Zheng, and A. Tadjeddine, Chem. Phys. **219**, 221 (1997).